Transient EHL Analysis of Helical Gears

Dr. Hazim Jamali, Dr. Kayri J. Sharif, Prof. Pwt Evans and Ray W. Snidle

This paper describes a transient, elastohydrodynamic lubrication (EHL) model of involute helical gears and examines the extent to which their behavior can be approximated using both equivalent point and line contact steady-state approaches. Significant transient effects are found near the ends of the contact line — particularly at locations where tip relief is active. Different tip relief profiles considered show that high stress concentrations and poor lubricant films may be avoided with suitable profile choice. Finally, 3-D results of a preliminary evaluation of surface roughness effects on local contact stress and EHL film thickness are presented.

Introduction

This paper addresses the lubrication of helical gears — especially those factors influencing lubricant film thickness and pressure. Contact between gear teeth is protected by the elastohydrodynamic lubrication (EHL) mechanism that occurs between non-conforming contact when pressure is high enough to cause large increases in lubricant viscosity due to the pressure-viscosity effect, and changes of component shape due to elastic deflection. Acting together, these effects lead to oil films that are stiff enough to separate the contacting surfaces and thus prevent significant metal-to-metal contact occurring in a well-designed gear pair.

EHL analysis of simple spur gear contact can be achieved with a straightforward line contact analysis, assuming plane strain conditions. For a helical gear pair, however, kinematic and geometrical conditions vary along the contact line; and if crowning of the teeth is applied, point contact analysis is required. Conditions change continuously through the meshing cycle, so there is a transient effect that should be included in the analysis.

As the gears rotate, a line of contact moves across the teeth; in general, there is more than one contact occurring at any given time. The number of simultaneous contacts and their total length depends upon the basic gear parameters, principally the base helix angle β_b and the face width, F (Fig. 1). The lines of contact are limited at their two ends — either by their intersection with the side edges of the gear, or at the tips of the teeth. Both of these locations are potentially zones of high-contact stress concentration and associated EHL film thinning. To avoid premature tooth engagement, "tip relief" is usually applied and the gear teeth may be "crowned" so that the contact area becomes an elongated ellipse under load. The effect of helical gear tip relief has been considered by Kahraman and co-workers (Refs. 1–2), for example. This paper considers the EHL consequences of tip relief. Details of the analysis techniques are given (Ref. 3), where previous EHL studies of helical gears using various simplified analyses are reviewed. This paper provides results for a full 3-D EHL treatment that takes account of both transient and side-leakage effects based on the detailed geometry of crowned and tip-relieved teeth.

EHL Modelling of Helical Gear Contact

The EHL model for the contacting gear teeth is developed in the plane containing the contact line that is perpendicular to the common normal of the contacting teeth. This is referred to as the common tangent plane as (Fig. 1). It is perpendicular to the plane of contact, which is tangential to the base cylinders of both gears and contains the contact line at all contact positions of the gear pair. The motion of the gear tooth surfaces relative to the contact line takes place in the tangent plane and the lubrication mechanism must be considered with regard to axes *xyz* in Figure 1, where *z* is the common normal direction, *y* is the contact line direction, and *xy* is the common tangent plane.

The 2-D, non-Newtonian Reynolds equation relating lubricant pressure, *p*, and film thickness, *h*, is:

$$\frac{\partial}{\partial x}\left(\sigma_x \frac{\partial p}{\partial x}\right) + \frac{\partial}{\partial y}\left(\sigma_y \frac{\partial p}{\partial y}\right) - \frac{\partial(\rho \overline{U} h)}{\partial x} - \frac{\partial(\rho h)}{\partial t} = 0 \tag{1}$$
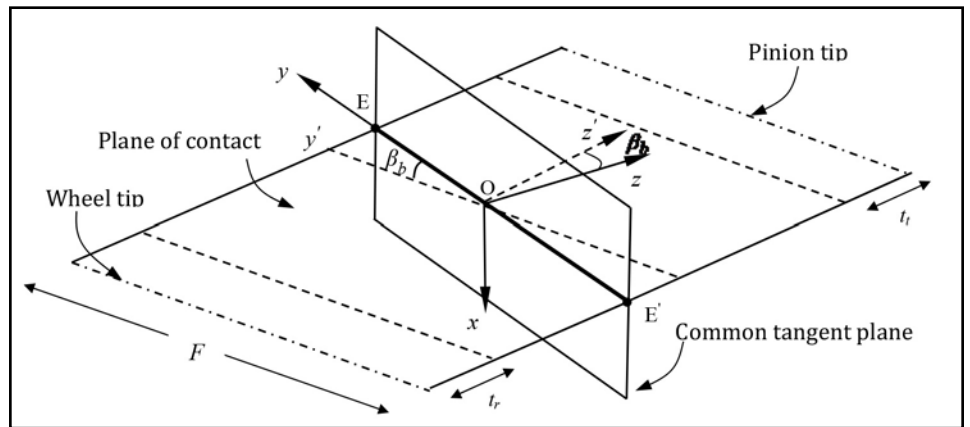

Figure 1   Plane of contact and common tangent plane intersecting on contact line EE' showing common normal direction, *z*, and tangent plane axes, *x* and *y*.

The lubricant entrainment velocity $\overline{U}$ is the mean velocity of the surfaces normal to the (*y*, *z*) plane, i.e. — in the *x* direction. The elastic deflection equation is written in a differential form (Ref. 4) as:

$$\frac{\partial^2 h(x_i,y_i)}{\partial x^2} + \frac{\partial^2 h(x_i,y_i)}{\partial y^2} = \nabla^2 (h_u(x_i,y_i)) + \frac{2}{\pi E'} \sum_{all\,k,\,all\,l} f_{k-i,l-j} p_{k,l} \tag{2}$$

Where, $f_{k,l}$ are weighting factors for the effect of pressure on the film thickness Laplacian. The time-varying EHL problem described by Equations 1 and 2 is analyzed using the technique described (Ref. 4), suitably modified to include the variation of load, kinematic and geometrical conditions during the meshing

cycle of the gears. In Equation 3 the terms σ_x and σ_x are:

$$\sigma_x = \frac{\rho h^3}{12\eta} S_x \cdots ; \cdots \sigma_y = \frac{\rho h^3}{12\eta} S_y \qquad (3)$$

Lubricant density and viscosity, ρ and η, are functions of pressure, and the non-Newtonian parameters S_x and S_y depend on h, η, $\partial p/\partial x$, $\partial p/\partial y$, and the sliding speed U_s.

To apply these equations to the gears, the undeformed gap between the contacting surfaces is required to give $h_u(x,y)$ in Equation 2. This is obtained by considering the distance s from the pitch line to each point of the contact line measured in the direction of z, and establishing the local radii of curvature of the involute profiles that are used to obtain the un-deformed gap h_u. Microgeometry corrections, such as axial crowning (to prevent contact extending to the face boundaries and consequent edge effects and stress concentrations) and involute profile tip relief (to prevent premature engagement of the teeth under loaded conditions), are added to h_u (Ref. 3).

With helical gears, the motion is transmitted gradually and smoothly between the mating gears, as opposed to spur gears where contact occurs along a straight line parallel to the gear axis. Contact starts as a point at the tooth face end and, as the gears rotate, this extends to become a line increasing steadily in length (e.g., line EE′, Fig. 1) until it starts to contract, finally ending as a point at the other tooth face. This gradual engagement and disengagement leads to the gradual, even action of the tooth and distribution of load. The lines of contact act diagonally between the face ends of the teeth and there are at least two pairs of teeth in contact during the meshing cycle. These factors allow helical gears to have increased load capacity, compared with the corresponding spur gear drive.

Results

Pressure and film thickness contour plots for each position in the meshing cycle can be obtained from the transient analysis. The gear pair considered in this paper has module 4.5 mm, tooth numbers 33 and 99, pressure angle 20° and reference helix angle 19.6°. The gears have a face width of 44 mm with pinion tip diameter 166.61 mm, wheel tip diameter is 481.83 mm, and center distance 315.22 mm. The maximum length of the contact line during the meshing cycle is $w = 46.7$ mm. The meshing cycle is analyzed in 575 time-steps covering the mesh positions where the contact line exceeds $0.16w$. The pinion torque used for the analysis was 1.06 kNm with a rotational speed of 235.6 rad/sec. The analysis was isothermal with $\eta_0 = 0.00625$ Pas; pressure-viscosity coefficient $\alpha = 13.3$ GPa^{-1}; and non-Newtonian shear thinning parameter $\tau_0 = 10$ MPa.

In the middle third of the meshing cycle the contact lines extend from one face to the other and the conditions are similar to those seen in an elliptical EHL point contact with a high-contact aspect ratio. In this case the contact dimensions in the y and x directions are in the ratio of about
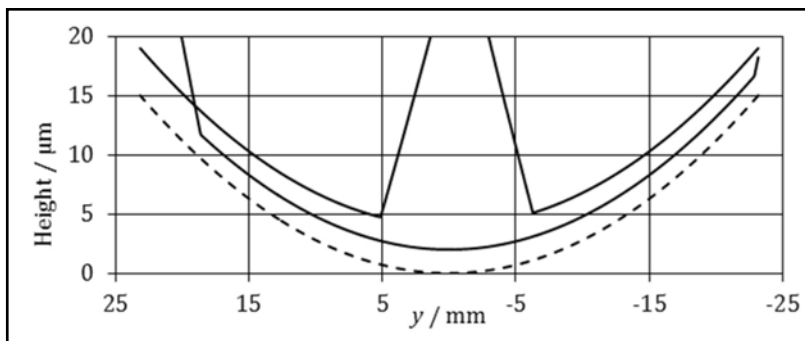

Figure 2   Gap between gear surfaces (offset) along contact line at positions 1, 2 and 3 in the meshing cycle with axial crown shown broken.

75:1. A characteristic horseshoe-shaped restriction is seen in the film thickness contour plot at the exit to the Hertzian zone and the pressure distribution is essentially Hertzian.

During the first part of the meshing cycle the effective contact line is limited by the tip relief profile applied to the wheel tooth, and during the latter part it is limited by the tip relief profile applied to the pinion tooth. Figure 2 illustrates the zero load gap between the tooth surfaces along the contact line at three meshing cycle positions.

Mesh positions 1, 2 and 3 are at time-steps 75, 300, and 500, respectively. In the figure the zero load gaps are offset by 2 or 4 μm for clarity. For position 2 it is clear that the gap is given by the axial crown, with the pinion tip relief becoming apparent for $y > 20.9$ mm. The tip relief profile illustrated in Figure 2 is linear. For position 1 the contact is essentially limited by the wheel tip relief at $y < 5.4$ mm, and for position 3 it is limited by the pinion tip relief for $y > -5.6$ mm. For positions 1 and 3 the combination of the axial crown and the active tooth relief leads to contacts that are curtailed at the onset of tip relief position where a significant stress concentration emerges in the calculations.

In all of the contacts there is a zone where the transient EHL result is essentially the same as the steady-state result for the geometry and kinematics at that position. This is illustrated in Figures 3, 4 and 5 for the three mesh positions that show sections of pressure and film thickness in the rolling/sliding direction. The figures show the steady-state 3-D results as solid lines and the transient results as broken lines. The equivalent 2-D line contact result is shown as a dash-dot curve for the sections where the transient and 3-D steady-state results are very similar.

The sections shown in Figures 3(a) and 3(b) show considerable differences between the transient and steady-state analyses in the vicinity of the tip relief profile modification. The pressure sections are almost identical, but the film thickness shows that the squeeze film terms in the Reynolds equation are active,
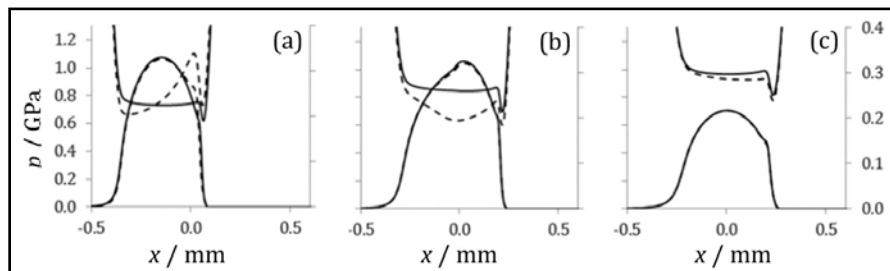

Figure 3   Pressure and film thickness sections at mesh position 1 for (a) $y=2$; (b) $y=5$; and (c) $y=12$ mm.
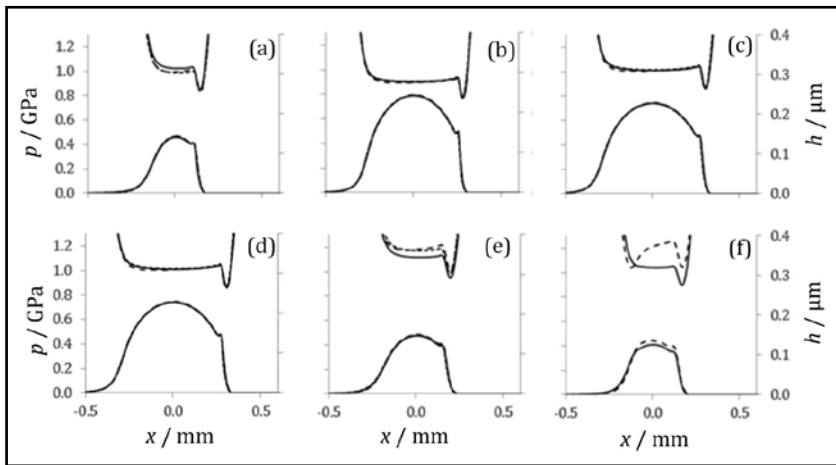
Figure 4 Pressure and film thickness sections at mesh position 2 for (a) $y = -18$; (b) $y = -10$; (c) $y = 0$; (d) $y = 10$; (e) $y = 17$; and (f) $y = 18$ mm.
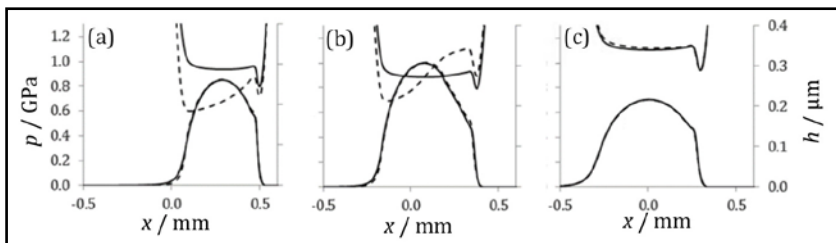

Figure 5 Pressure and film thickness sections at mesh position 4 for (a) $y = -2$; (b) $y = -5$; and (c) $y = -10$ mm.
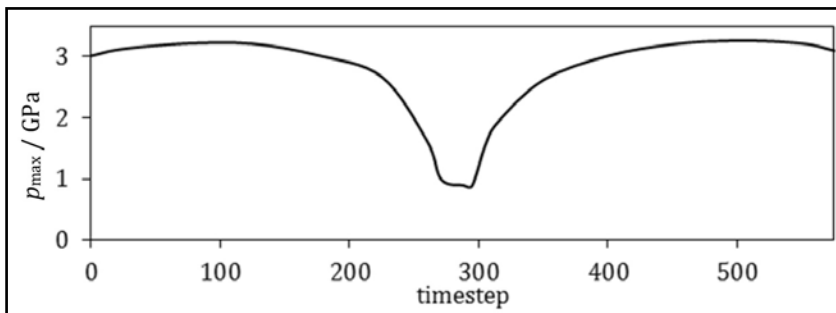

Figure 6 Maximum pressure obtained in each time-step for the case of linear tip relief profile.
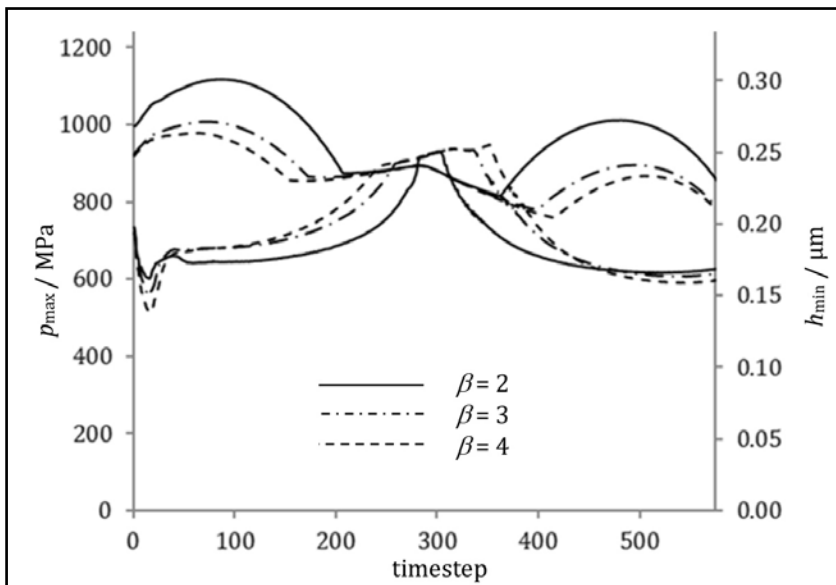

Figure 7 Maximum pressure (upper curves) and minimum film thickness (lower curves) over the meshing cycle

causing significant differences in the lubricant films. For Figure 3(c), which is typical of the rest of the contact line, the transient and steady-state results are very similar, showing that the squeeze film term is not influential when away from the tip relief position.

Figure 4 shows that in mesh position 2, the contact behaves in the same way as its steady-state counterpart for most of the contact length, with the only significant transient effects being seen in the film thickness profile of Figure 4(f), where squeeze film effects are active at the location of active tip relief. For sections 4(a) to 4(e), equivalent 2-D line contact analyses are also included that can be seen to show the same behavior.

Figure 5 shows results that are similar to those for Figure 2 in that steady-state behavior is apparent in Figure 5(c), which is representative of most of the contact line, with significant transient effects in Figures 5(a) and 5(b) that are in the vicinity of the tip relief profile modification. Again, the pressure sections are almost identical, with significant film thickness differences due to squeeze effects.

Figure 6 shows the maximum pressure obtained during the meshing cycle when the tip relief profile adopted is linear. The gears are operating at a nominal maximum Hertzian pressure of about 0.9 GPa, and it can be seen that during full contact width operation this is representative of the maximum pressure experienced. However, during the parts of the meshing cycle where the tip relief profile limits the length of contact, very high pressures of up to 3.5 GPa are experienced and the fluid film is unable to completely separate the surfaces (Ref. 3).The high-pressure levels are due to the stress concentration caused by the tip relief profile. This is discussed (Ref. 3) where the nature of the tip relief profile was varied by including a parabolic transition between the involute profile and the linear tip relief so that the slope of the tooth flank remained continuous.

In the current study the tip relief is taken to be in the form of the power law

$$z_t = c_t \{(r - r_{start})/(r_t - r_{start})\}^{\beta} \qquad (4)$$

where r is the radius from the gear axis, r_{start} is the start of tip relief radius, r_t is the tip radius, and c_t is the profile removed at the tip. The value of parameter β is varied between 1 and 4, where $\beta = 1$ corresponds to the linear profile.

Figure 7 shows the variation of maximum pressure and minimum film thickness over the meshing cycle for values of $\beta = 2$, 3 and 4. The maximum pressures are reduced by a factor of three or more when compared to the result for $\beta = 1$ (Fig. 6). The value of β can be seen to have a significant effect on the peak pressures and also on

the minimum film thickness experienced in the contact. The pressures are further reduced for the higher β values, but these are minor additional changes.

Figure 8 shows film thickness and pressure contours at time-step 75 for the range of powers β specified for the analyses. For the linear profile $\beta = 1$, the maximum pressure contour is 3.2 GPa and the minimum film thickness contour is zero, indicating that the lubricant film is unable to separate the surfaces. This extreme behavior is not seen with the cases where $\beta = 2$, 3 and 4, where the minimum film thickness contours are around 0.185 μm and the maximum pressure contour values are 1.1, 1.0 and 0.96 GPa, respectively.

Figure 9 shows the contact line pressures for each time-step assembled into a contour plot for each of the tip relief profile forms considered. For the $\beta = 1$ case, intense closed contours for 3, 2 and 1 GPa appear at the top and bottom of the pressure map. The y axis is aligned with the contact line and the peak pressure contour indicates that the highest pressures occur at the start of tip relief positions, on the wheel at the bottom left of the contour plot, and on the pinion at the top right. For the higher values of β these contours become much less intense and the peak contact line pressure levels approach those occurring at the peak load full face width contact lines.

For the parts of the contact lines that operate in steady-state mode, a 3-D line contact analysis has been developed that allows consideration of the surface roughness present on both helical gear surfaces (Ref. 5). This analysis uses fast Fourier transforms (FFTs) to evaluate the surface deflection due to the pressure distribution (i.e., the last term of Eq. 2) and exploits the aliasing error introduced by the finite discrete FFT to consider a rectangular x-y solution space where x is the rolling/sliding direction, and y is in the direction of the contact line. Representative surface roughness profiles are introduced that are subject to periodic flow boundary conditions at the transverse, y, boundaries. The resulting solution corresponds to a line contact with surface roughness that is repeated periodically in the y direction. This enables the representative roughness to be extruded, either in the contact line direction (Fig. 11) or at appropriate inclinations to the contact line, which is currently a work in progress.

Figures 10 and 11 show results from 3-D line contact analyses. Figure 10 considers smooth surfaces extruded in the y direction The Hertzian line contact dimension for the case presented is 0.25 mm, and tests were carried out to establish the appropriate y dimension for the 3-D model to give the correct 2-D line contact result. It was found that using a y dimension of 1 mm or more yields 3-D results that are identical to the 2-D result. Smaller values of the y dimension give 3-D results that vary in the y direction.
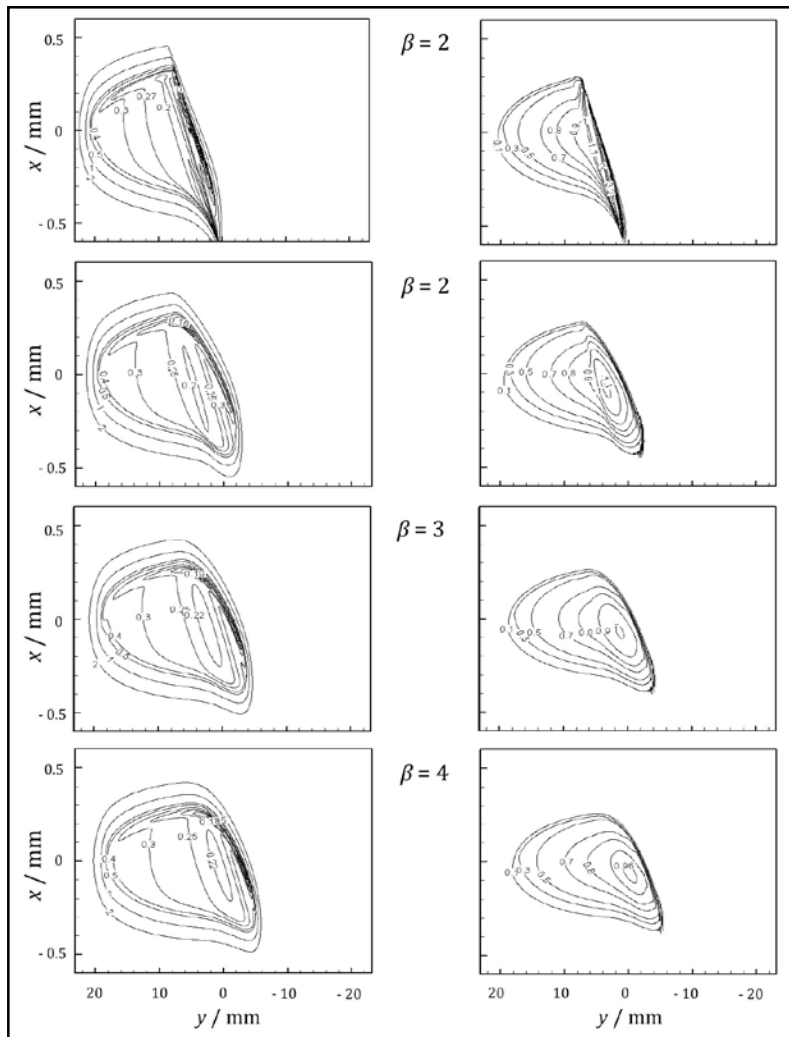

Figure 8 Film thickness contours/μm (left) and pressure contours/GPa (right) at timestep 75 for the four values of β.
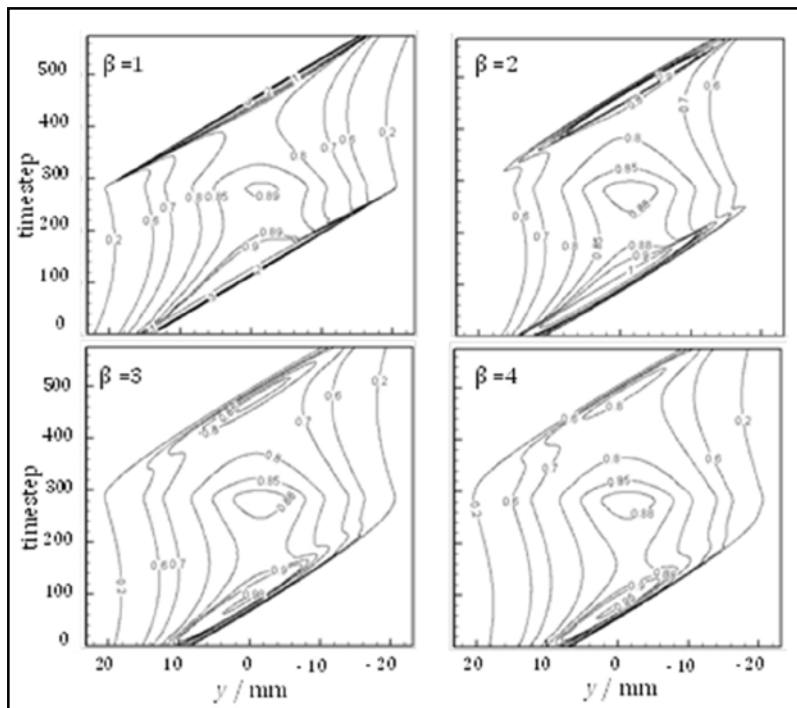

Figure 9 Contours of contact line pressure/GPa for the four values of β.
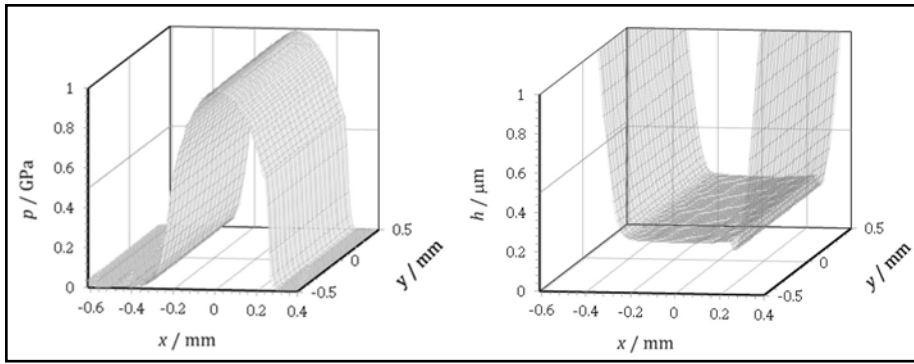
Figure 10   Pressure (left) and film thickness (right) results for a 3-D line contact with smooth surfaces.

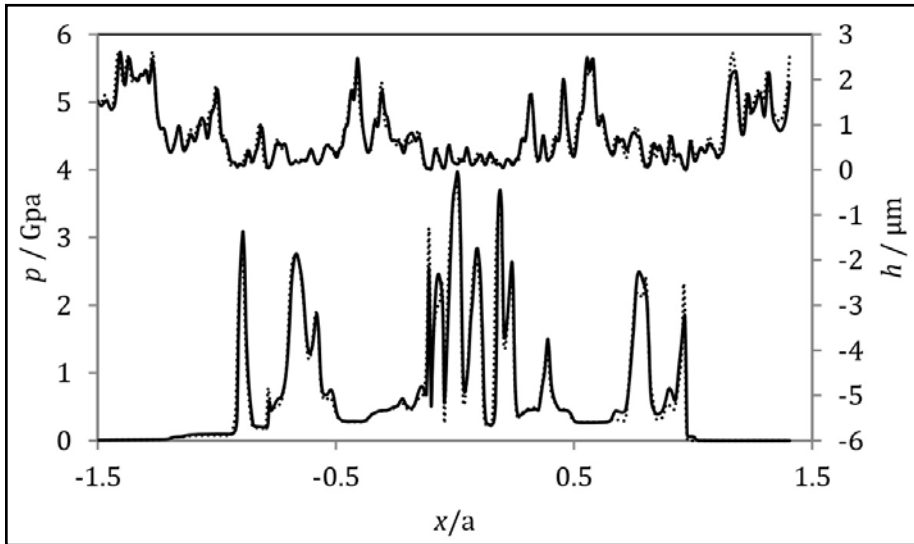**Figure 11   Pressure (lower curves) and film thickness (upper curves) for a time-step for 3-D (solid) and 2-D (dashed) analyses with rough surfaces.**

analysis gives the same pressure and film thickness response.

The tip relief profile adopted is very influential in determining the maximum pressure experienced by the gear flanks. Linear relief profiles lead to a significant stress concentration, together with extremely adverse film-forming conditions at the transition between the involute and relieved profile. This is because the linear tip relief introduces a slope discontinuity in the form of a cusp to the tooth geometry. However, these effects can be limited provided that the material removal to provide tip relief does not introduce a slope discontinuity.

A 3-D line contact approach is discussed as a means of introducing a surface texture that is periodic in the contact line direction into the EHL model.

Figure 11 compares the results for a single time-step from a 3-D transient line contact analysis with two rough surfaces whose roughness profiles are extruded in the *y* direction. The line contact analysis is presented with dashed lines that can be seen to replicate the 3-D analysis almost exactly. This approach can therefore be used to examine the effects of surface texture in helical gears. It is important to note that the boundary conditions applied must allow transverse flow at the limits of the model in order to properly represent the EHL flow in the helical gear contact, which was not the case in (Ref. 5). This limits the textures that can be considered to those consistent with applying periodic normal flow boundary conditions at the transverse boundaries.

Conclusions
Comparison of transient EHL analyses for the whole tooth contact with steady-state analyses using the instantaneous tooth geometry and kinematics show that transient effects are limited to the areas close to the ends of the contact lines where contact is limited by tip relief. For the bulk of the load carrying area the gears considered can be approximated by a sequence of steady-state analyses. Furthermore, for the areas that behave in this way, the aspect ratio of the contact is such that a line contact

References
1. Wagaj, P. and A. Kahraman. "Influence of Tooth Profile Modification on Helical Gear Durability," *Trans. ASME in Mechanical Design,* Vol. 124, 2002, Pp. 501–510.
2. Kahraman, A., P. Bajpai and N.E. Anderson. 2005, ''Influence of Tooth Profile Deviations on Helical Gear Wear," *Trans. ASME in of Mechanical Design*, Vol. 127, 2005, Pp. 656–663.
3. Jamali, H. U., K.J. Sharif, H.P. Evans and R.W. Snidle. "The Transient Effects of Profile Modification on Elastohydrodynamic Oil Films in Helical Gears" (under review); *Tribology Transactions*, 2014.
4. Holmes, M. J. A., H.P. Evans and R.W. Snidle. "Analysis of Mixed Lubrication Effects in Simulated Gear Tooth Contacts," *Trans. ASME in Tribology*, Vol 127, 2005, Pp. 61–69.
5. Ren, N., D. Zhu, W.W. Chen, Y. Liu and Q.J. Wang. "A Three-Dimensional, Deterministic Model for Rough Surface, Line Contact, EHL Problems," *Trans ASME in Tribology*, Vol.131, 2009, pp 1-9.

Dr. Hazim Jamali is a faculty member of the college of engineering at the University of Karbala, Iraq; he studied mechanical engineering at the University of Baghdad, where he was awarded B.S. and M.Sc. degrees. He recently completed his doctoral studies at the Cardiff School of Engineering, Cardiff University where he was awarded a Ph.D. for his thesis — "Analysis of Helical Gear Performance Under Elastohydrodynamic Lubrication." Jamali's principal research interest is in gear technology and numerical analysis, and he has in fact authored several papers in this area of study.

Dr. Kayri Sharif holds BSc and MSc degrees in mechanical engineering from the University of Bagdad, where his masters project work introduced him to the field of tribology. He was awarded a PhD by Cardiff University for research in dynamic performance of machine tool spindle bearing systems. He is a member of the IMechE (Institution of Mechanical Engineers) and a chartered engineer. Currently he is a senior research associate at the Cardiff School of Engineering where he is a member of the tribology and contact mechanics research group. Sharif has worked extensively on software development for modelling EHL contacts in machine elements of various kinds, and has authored 37 technical papers addressing issues in tribology and machine dynamics.

Professor Pwt Evans leads the tribology and contact mechanics research group at the Cardiff School of Engineering. He received his higher education at the University of Exeter, from which he holds BSc, PhD and DSc degrees. He is a chartered engineer and a Fellow of both the Institution of Mechanical Engineers and the Learned Society of Wales; he was awarded the Tribology Trust Silver medal in 2009. He has researched in the field of elastohydrodynamic lubrication since his post-doctorate research, where he produced the first point contact EHL solutions at realistic engineering loads. He has worked on a range of projects with many companies — mainly in the EHL field — and has published some 150 technical papers in this area. His main interests are in mixed lubrication and micropitting in gears, but he also has interests in plain bearings and in self-lubricating, composite liner bearings.

Ray Snidle is a (semi-retired) professor of mechanical engineering at Cardiff University where he contributes to the tribology and contact mechanics research group. A chartered engineer and Fellow of both IMechE and ASME, he holds PhD and DSc degrees from Leicester University prior to his obtained industrial experience at Rolls-Royce Aircraft Engines, Bristol. His dominant research interests are in the field of the tribology of gear tooth contacts, with particular emphasis on the failure of elastohydrodynamic lubrication (EHL) leading to scuffing and micropitting.